This is a repository copy of *Determination of Retrogradation Degree in Starch by Mid-infrared and Raman Spectroscopy during Storage*.

White Rose Research Online URL for this paper:
https://eprints.whiterose.ac.uk/179324/

Version: Accepted Version

Article:

Determination of retrogradation degree in starch by Mid-infrared and Raman spectroscopy during storage

Xuetao Hu[a, c, d], Jiyong Shi[a, c, d], Fang Zhang[a], Xiaobo Zou[a,c,] *, Mel Holmes[b, c], Wen Zhang[a], Xiaowei Huang[a], Xueping Cui[a], Jin Xue[a]

[a]Key Laboratory of Modern Agriculture Equipment and Technology, School of Food and Biological Engineering, Jiangsu University, Zhenjiang 212013, China

[b]School of Food Science and Nutrition, the University of Leeds, Leeds LS2 9JT, United Kingdom

[c]Joint Laboratory of China-UK on food nondestructive sensing, Jiangsu University, Zhenjiang 212013, China

[d] Contributed equally to this work

*Corresponding author.

Tel: +86 511 88780085; Fax: +86 511 88780201

Email address: zou_xiaobo@ujs.edu.cn (Xiaobo Zou)

Abstract

Retrogradation behavior is an important physicochemical property of starch during storage. A fast and sensitive method was developed for determining the retrogradation degree (RD) in corn starch by mid-infrared (MIR), Raman spectroscopy and combination of MIR and Raman. MIR and Raman spectra were collected from different retrogradation starch and then processed by partial least-squares (PLS), interval PLS (iPLS), synergy interval PLS (siPLS), and backward interval PLS (biPLS). Two different levels' fusion data extracted from MIR and Raman spectra were analyzed by partial least-squares (PLS). The developed models demonstrated that both MIR and Raman techniques combined with chemometrics can be used to determine the RD in starch. The PLS model built by medium-level fusion approach achieved the most satisfied performance with a correlation coefficient of 0.9658. Integrating MIR and Raman technique combined with chemometrics improved the prediction performance of RD in comparison with a single technique.

Keywords: Retrogradation degree; Starch; Raman spectroscopy; MIR spectroscopy; Partial least-squares

Introduction

Starch presented in an enormous variety of food products acts as the main materials to supply nutrition and energy, or as an additive to improve the quality of food. Starch retrogradation behavior is an important physicochemical property of starch during storage. Retrogradation could lead to deterioration of starch-based food during storage (Eliasson 2010), while retrogradation also could provide starch food with functional properties. Starch is beginning to retrograde after starch completely gelatinized. During retrogradation, molecular chains in starch begin to reassemble to develop an ordered structure (Ferrero et al. 1994). Generally, starch paste retrogradation is accompanied by gradual increases in rigidity and phase separation between polymer and solvent (Karim et al. 2000). Starch-based foods after retrogradation are indigestible by body enzymes and may make consumer suffer from indigestion (Hayakawa et al. 1997). Therefore, a number of steps were attempted to study and prevent retrogradation (Liu et al. 2007). As we all know, one kind of resistant starch called RS_3 is the retrograded starch forming during cooling of gelatinized starch. As a new resource of dietary fiber, retrogradation starch can provide functional properties and find applications in a variety of foods (Karim et al. 2000; Sajilata et al. 2006). Consumers prefer appropriate retrogradation to no retrogradation in starch-based products. Retrogradation is used to harden products and reduced products stickiness during the manufacturing process of breakfast cereals and parboiled rice (Karim et al. 2000). The retrogradation starch is often said that

53   retrogradation deteriorates the quality of starch food. It is equally true that the suitable

54   retrogradation starch is a benefit to gastrointestinal digestion. Therefore, the

55   retrogradation degree (RD) in starch is a very important index for monitoring the

56   quality of starch foods.

57   Various methods have been applied for studying retrogradation starch, such as

58   rheological methods texture profile analysis (TPA) and rapid visco analyzer (RVA)

59   (Mariotti et al. 2009; Olayinka et al. 2011), thermal analysis (differential scanning

60   calorimetry (DSC), differential thermal analysis (DTA) and nuclear magnetic

61   resonance (NMR))(Chang and Liu 1991). The most popular method is enzymatic

62   methods based on acid or amylolytic enzymes (e.g. *a-amylase* and *β-amylase* etc.) for

63   determining RD in starch. Normally, the RD is measured by determining residual non-

64   digestible starch which is not digested to glucose after incubation with amylolytic

65   enzymes (Karim et al. 2000). These methods are complicate, laborious and time-

66   consuming. Rheological methods are used to evaluate the characteristics of

67   retrogradation starch based on viscosity property, hardness and elasticity (Karim et al.

68   2000). These properties can provide the qualitative description of starch

69   retrogradation while the RD values was not determined specifically (Smits et al.

70   1998). The enthalpy in the melting endotherm resulting from thermal analysis was

71   used as the index for evaluation of starch retrogradation (Paker and Matak 2016).

72   Samples detected by thermal analysis, enzymatic methods and rheological methods

73   are not reusable by consumers (Chang and Liu 1991). Most NMR instruments are

74   expensive and not available in many labs or industries (Monakhova and Diehl 2016).

75   Spectroscopic methods have been used in study of retrogradation as

76   nondestructive methods, such as near-infrared (NIR) spectroscopy, mid-infrared

77   (MIR) spectroscopy, Raman spectroscopy, and so on (de Peinder et al. 2008; Rocha et

78   al. 2016; Thygesen et al. 2003). Each retrogradation starch has a unique and

79   characteristic spectrum due to their particular molecular component and structure.

80   NIR shows overtones and combination vibrations of the molecule when NIR beam

81   irradiates into samples. The molecular bands observed in NIR spectra are very broad

82   resulting in that it is difficult to ascribe specific bands to specific chemical

83   components (Romano et al. 2016). Both MIR and Raman spectroscopy can generate

84   bands linked to fundamental vibration and supply fingerprints of components that can

85   be used for quantitative and qualitative characterization (Vankeirsbilck et al. 2002).

86   They have been applied to characterize the molecular structural changes of

87   retrogradation starch, and are conducive to comprehending the changes of amylose

88   and amylopectin (Flores-Morales et al. 2012). However, there is no study about

89   quantitative analysis of RD in starch by MIR, Raman and the combination of them.

90   Different types of starch (from pure corn and cassava starch samples, as well with

91   mixtures from both starch types) can be characterized usin by using Raman

92   spectrscopy(Almeida et al. 2010). Besides Raman spectroscopy, MIR spectroscopy

93   can also be used for quantitative analysis of RD in starch (Wu et al. 2016). Acting as

94   complementary spectroscopic techniques, both types of measurements, Raman and

95 MIR, can provide different molecular vibrations. (Thygesen et al. 2003). Previous

96 studies have demonstrated that data fusion technique based on MIR and Raman can

97 increase the prediction ability of chemical components in food (Wu et al. 2016). .

98   Therefore, the objectives of this paper were: (1) to use MIR, Raman

99 spectroscopy and the combination of two techniques for investigating the

100 retrogradation behavior in starch; (1) to establish a nondestructive and rapid method

101 for measuring the quality, acceptability, and shelf-life of starch-containing foods.

102 **Materials and methods**

103 **Retrogradation starch preparation**

104   Corn starch was purchased from Runzhou Starch Company in Zhenjiang. A

105 solution of corn starch (1g) suspended in 19 ml of water was heated at 100℃ with

106 constant stirring for 1 hour in order to make starch completely gelatinized. The

107 gelatinized starch paste was stored for different time (0, 1, 2, 3, 4, 5, 10, 15, 20 days)

108 at 4℃. After storage, retrogradation starch with different storage time was dried and

109 kept in a desiccator. Sixteen samples for each retrogradation starch were prepared

110 using same procedures. All samples were obtained from one independent

111 gelatinization experiment.

112 **MIR and Raman spectroscopy**

113   The MIR spectra of retrogradation starch were collected by Nicolet 380 FT-IR

114 spectrometer (Thermo Electron Corporation, USA) in the spectral range of 650 to

115 4000 cm^{-1} at resolution of 2 cm^{-1} (Flores-Morales et al. 2012). Raman spectra were

116   recorded with DXR Laser micro-Raman spectrometer (Thermo Electron Corporation,

117   USA) with 532 nm laser source. During collection of Raman spectra, time of

118   integration is 5 seconds. For each spectrum, an average of 32 scans were performed at

119   a resolution of 1 cm^{-1}, over the 100-3200 cm^{-1} range (Xu et al. 2014). To obtain the

120   most useful spectral information, multiple scans were performed in different points of

121   the sample by moving the substrate on an X-Y stage. And the spectra from same

122   sample were averaged into one spectra. Before collection, the Raman system was

123   calibrated with a silicon semiconductor. The laser power irradiation over the samples

124   was 4 mW. Finally, 144 and 144 spectra for MIR and Raman were obtained,

125   respectively.

126   **Reference analysis of RD in starch**

127   The reference RD in starch was measured by the modified method of *Tsuge* et al

128   (Di Paola et al. 2003). A solution of 25 mg retrogradation starch in 8 ml distilled water

129   was placed into a test tube. 5 ml 0.1 mol L^{-1} phosphate buffer (pH 6.0, 0.3% NaC1)

130   and 2 ml 3.5u ml^{-1} α-amylase solution was then placed into the test tube. After

131   incubation for 1 hour at 37°C, the enzymatic reaction was stopped by adding 5ml of 4

132   mol L^{-1} NaOH. The pH of the solution was adjusted to neutrality with 4 mol L^{-1} HC1

133   and the volume was made up to100 ml with distilled water. 5 ml of iodine solution

134   (0.2% I$_2$-2% KI) was added to l0 ml of the digested solution, and made up to l00 ml

135   with distilled water. The absorbance of solution at 625 nm was measured after

136   standing for 20 min. The RD (%) is calculated from equation described by *Tsuge* et al.

137   The values of RD obtained would be used for the construction and validation of

138   model (Kim et al. 1997).

139   **Data analysis**

140   Different pre-processing techniques (standard normal variate (SNV), mean

141   centering (MC) and multiplicative scatter correction (MSC), Savitzky–Golay

142   smoothing (SG)) were applied for eliminating baseline shift and scatter effects etc. By

143   comparing results obtained from four preprocessing methods, SG is much better than

144   SNV, MC and MSC (Chen et al. 2011).

145   PCA was performed to show the clustering trend of retrogradation starch samples

146   (Yeung and Ruzzo 2001). PCA is a well-known method for feature extraction in

147   spectral analysis. It transforms the original independent variables into new variables

148   (principal components (PCs)). The PCs are orthogonal and can be used as input

149   variables for pattern recognition analysis (Haiyan et al. 2008).

150   Partial least squares (PLS) is used extensively for it is able to cope with high-

151   dimensional data by extracting latent variables. So far, PLS has been widely used to

152   build multivariate calibration models using the whole spectrum (WS) range (Lin et al.

153   2016). Therefore, WS-PLS models based on MIR spectra or Raman spectra were

154   established. In application of PLS algorithm, the optimum number of latent variables

155   (*LVs*) are a critical parameter in calibration model.

156   Interval variable selection algorithms (iPLS, siPLS, and biPLS) proposed based

157   on the PLS method were used to eliminate uncorrelated variables to improve PLS

model performance(Chen et al. 2008). Literatures have discussion about the important variables selection or unimportant variables elimination(Zou et al. 2007; Ma et al. 2017). The principles of interval variable selection algorithms were described in various papers(Ma et al. 2017). In iPLS algorithm, the *RMSECV* was calculated for every subinterval when the full spectrum was split into 40 intervals. The spectral region with the lowest *RMSECV* was chosen as the best interval for prediction of RD. In siPLS and biPLS algorithm, the combination of intervals with the lowest *RMSECV* is chosen(Chen et al. 2008). This enables us to select the best combination of intervals, generally providing better correlation coefficient (*R)* values and smaller prediction errors than iPLS(Nørgaard et al. 2000).

PLS models based on fusion data extracted from MIR and Raman spectra were investigated. Fusion data were carried out basically at three level: low-level fusion, mid-level fusion and high-level fusion(Borràs et al. 2015). High-level fusion has often provided worse results than the other two levels(Nunes et al. 2016). Thus, low- level fusion and medium-level were investigated in this paper(Wu et al. 2016). Low-level fusion data consists of original variables of MIR and Raman after the preprocessing steps. Medium-level fusion extracts relevant features from MIR and Raman data separately and then merges them into a single matrix, which will be analyzed by chemometrics (Borràs et al. 2015). In this paper, the characteristic intervals of MIR and Raman were combined as fusion data which acted as input data for establishing models.

179   144 MIR spectra were divided into two subsets which were called calibration set

180   and prediction set. The calibration set contained 90 spectra were used for establishing

181   model, and remaining 54 spectra as prediction set were used to test the performance of

182   predictive models. The 144 Raman spectra were processed like MIR spectra. In this

183   study, WS-PLS, iPLS, siPLS and biPLS models based on MIR or Raman spectra were

184   obtained. The low- and medium-level fusion approaches were applied to combine of

185   MIR and Raman. In all models, optimum number of latent variables (*LVs*) were

186   determined by root mean square error of cross-validation (*RMSECV*). The

187   performance of the final models were evaluated in accordance with the correlated

188   coefficient of determination (*R*), and *RMSEP* values (Varliklioz Er et al. 2016). The

189   data were processed in MATLAB software version 7.10 (Math Works, Natick, MA,

190   USA).

191   **Results and discussion**

192   **RD in starch stored for different time**

193   Corn starch was completed gelatinized as described in the experimental section

194   and then the starch pastes stored at 4 ℃ for 0, 1, 2, 3, 4, 5, 10, 15 and 20 days were

195   dried. Finally, nine kinds of retrogradation starch were obtained and named 0, 1, 2, 3,

196   4, 5, 10, 15 and 20 d. RD of retrogradation starch was determined by the enzymatic

197   method based on *α-amylase*. Average values of RD for nine kinds of retrogradation

198   starch were 15.87%, 45.64%, 67.21%, 77.39%, 85.30%, 91.05%, 94.91%, 97.07%,

199   and 98.73% shown in Fig. 1. The stand deviations of each kind retrogradation starch

200 were 1.234, 1.322, 0.9814, 1.097, 1.501, 0.5618, 0.5222, 0.5189, and 0.3777. It is

201 indicated that RD in starch increased with the storage time prolonged. RD at the first

202 five days varied significantly from 15.81% to 85.30%. The speed of retrogradation

203 was decreased gradually after 5 days. Particularly, the RD of 15 d and 20 d were

204 similar. It can be concluded that the structure and component of retrogradation starch

205 at 0, 1, 2, 3, 4 and 5 d alter dramatically while that at 10, 15, and 20 d alter slightly.
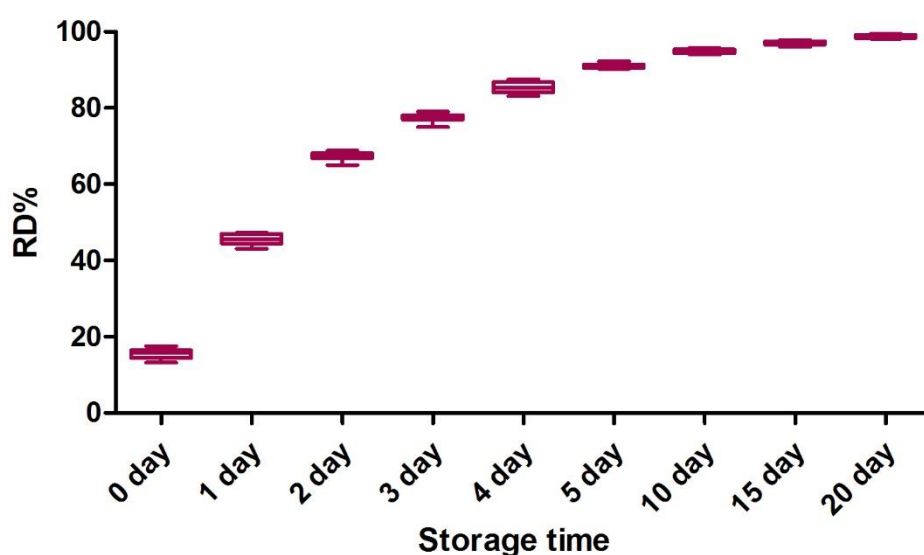
206
207 Fig. 1 retrogradation degree of corn starch paste stored for 1, 2, 3, 4, 5, 10, 15 and 20 days

208 **Spectral analysis**

209 MIR and Raman spectroscopy can be used to detect properties of retrogradation

210 starch, such as crystallinity and amorphization. Fig. 2 (a) shows the average MIR

211 spectra of retrogradation starch stored for 0, 1, 2, 3, 4, 5, 10, 15, and 20 days. Fig. 2

212 (b) shows average Raman spectra for the retrogradation starch samples with different

213 storage time.

214 MIR spectral patterns of retrogradation starch showed almost identical

215 characteristic bands (Fig. 2 (a)). The characteristic bands mainly contain 756, 820,

11

216   850, 880, 928, 949, 994, 1022, 1067, 1077, 1133, 1150, 1181, 1241, 1340, 1506,

217   1560, 1648, 1654, 1701, 2177, 2926, and 3275 cm^{-1}. These bands mainly resulted

218   from the vibrational modes of molecule in retrogradation starch. The bands around

219   1600 cm^{-1} are attributed to amorphous region of starch (Smits et al. 1998). The band

220   at 1506 cm^{-1} is influenced by the skeletal mode vibration of a-1, 4 glycosidic linkage

221   (C–O–C). The bands at 1022 and 850 cm^{-1} are sensitive to changes in crystallinity.

222   The nine Raman spectra for retrogradation starch also showed almost identical

223   characteristic bands (Fig. 2 (b)). The main vibrational bands of each spectrum are

224   similar because different samples contain the same main components

225   (polysaccharide). The vibrational bands mainly included 373, 408, 437, 480, 577, 860,

226   940, 952, 1051, 1082, 1126, 1260, 1338, 1382, 1462, 1518, 2116, 2870, 2908 cm^{-1}.

227   The band at 2908 cm^{-1} is related to the symmetrical and antisymmetric CH stretching.

228   The unobvious and sharped characteristic band at 2870 cm^{-1} can be attributed to the

229   amylose and amylopectin presented in starch(Kizil et al. 2002). The region between

230   1200 and 1600 cm^{-1} contain a large supply of structural information. A majority of the

231   bands in this region are due to coupled vibration involving hydrogen atoms. For

232   instance, the band at 1462 is related to CH, CH$_2$, and COH deformation. The feature

233   at 1382 cm^{-1} corresponds to coupling of the CCH and COH deformation modes. The

234   bands at 1260 and 1338 cm^{-1} can be mainly attributed to several vibrational modes,

235   such as CO stretching, CC stretching, CCH deformation, COH deformation, and CCH

236   deformation. The region between 1200 and 800 cm^{-1} is highly characteristic bands

owing to CO stretching, CC stretching and COC deformation modes, referring to the

glycosidic bond (Mahdad-Benzerdjeb et al. 2007). This region is considered as the

fingerprint or anomeric region, and is discussed with high frequency in the previous

papers (Baranska et al. 2005; Nikonenko et al. 2005; Yang and Zhang 2009).The

vibrations originating from glycosidic linkages can be observed in the 920-960 cm^{-1}

region. Particularly, the band observed at 940 cm^{-1} is assigned to the amylose α-1, 4

glycosidic linkage. Raman spectra of retrogradation starch exhibited complex

vibrational modes at low wavenumbers (below 800cm^{-1}) due to the skeletal mode

vibrations of the glucose pyranose ring. Among the Raman bands at 437, 480, 577, a

strong band at 480 cm^{-1} portraying the rate of polymerization in polysaccharides is

one of the prominent and important indication of the presence of pyranose ring due to

skeletal vibration mode(Kizil et al. 2002). Characteristic vibrational bands found in

retrogradation starch are shown in Table 1 for both IR and Raman.

Each spectrum of retrogradation starch is unique owing to its particular

component and structure. MIR peaks at 1047 and 1022 cm^{-1} have been used for

investigating changes in starch structure (organized starch and amorphous starch)

during starch retrogradation(Flores-Morales et al. 2012). Previous studies have shown

the most useful Raman bands which reflect the characteristics of retrogradation starch.

For instance, according to W.T. Winter et.al (Winter and Kwak 1987), intensity of the

Raman band at 480 cm^{-1} and the half-bandwidths of Raman bands at 2800-3000 cm^{-1}

were used as excellent indexes for evaluating retrogradation starch. Besides the bands

258   discussed in the previous work (Kizil et al. 2002), the intensities and shapes of other

259   characteristic bands are also relevant to the starch component and structure. However,

260   these bands were ignored for determination of retrogradation of starch. Therefore, the

261   more spectral feature will be applied for determining retrogradation starch in further

262   analysis.
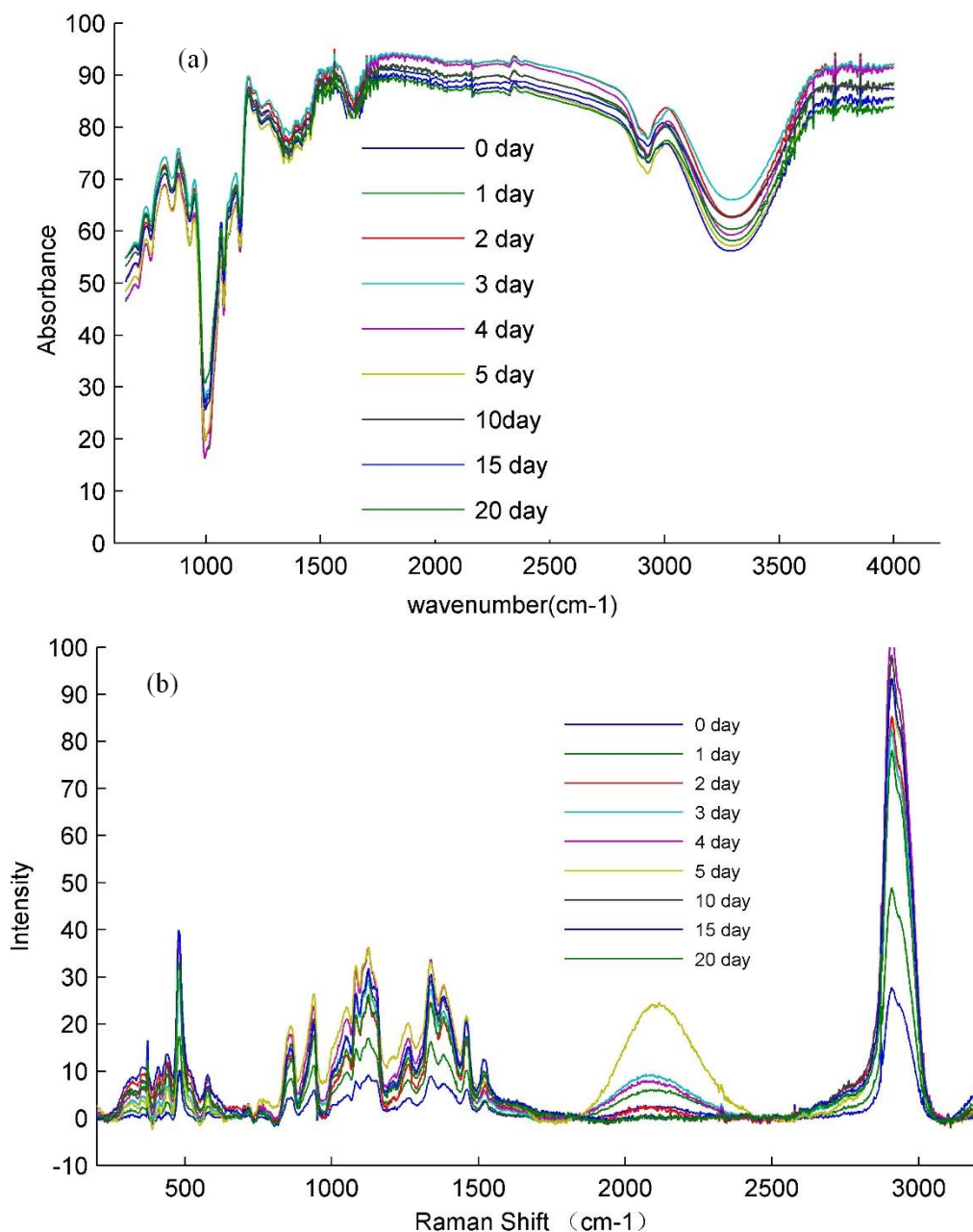
263
264   Fig. 2 mid-infrared and Raman spectra of different retrogradation starch

265 Table 1 IR and Raman wavenumbers and their respective tentative assignments based on literature data

IR (cm^{-1})	Assignments	Raman (cm^{-1})	Assignments
3275 S	ν(OH)		
2926 M	ν(CH)	2908 S	ν(CH)
1506 W	COC	1462 M, 1518 W	δ(CH) + δ(COH) + δ(CH$_2$)
1241 M	δ(CH) + δ(OH)	1338 S, 1260 M, 1382 M	δ (CH)
1150 S	ν(CO) + ν(CC)	1126 S	δ(COH) + ν(CO) + ν(CC)
1077 S, 1022 S	ν(CO) + ν(OH) + ν(CC)	1051 M, 1082 M	δ(COH) + ν(CO)+ ν(CC)
994, 928 W	γ(COOH) + δ(COO)	940 S, 952 S	δ(COC) + δ(COH) + ν(CO)
850 W	δ(CCH) + δ(COH) + γ(COH)	860 W	ν(COC) + ν(CCH)
		577 W	δ(CCO) + δ(CO)
		437W, 480 S	δ(CCO) + δ(CCC)

266 **General discrimination of Samples**

267   PCA was applied to MIR and Raman spectra to evaluate their ability to

268 differentiate the retrogradation starch with different storage time. The scores plots of

269 PCA for retrogradation starch stored 0, 1, 2, 3, 4, 5, 10, 15, 20 days were shown in

270 Fig. 3 (a) and (b). Fig. 3 (a) shows the scores plot of PCA based on MIR spectra. The

271 retrogradation starch samples were divided into two categories with some

272 overlapping. The first one category located at the left of the scores plot contained

273 retrogradation starch samples stored 0, 1, 2, 3 and 4 days. The starch samples stored 5,

274 10, 15 and 20 days belonged to the second category located at the right of the scores

275 plot. According to the RD determined by enzymatic method, the RD reached 85%

276 when the starch was stored 4 days. The average growth rate of one day was 21.25%.

277 The RD during the first four days increased rapidly. When the starch was stored for 20

278 days the RD of starch achieved 99%. From the 5th to 20th day, the RD increased from

279 85% to 99% with growth rate of 14%. The average growth rate of every day was

280 0.875%. The RD increased slowly. The starch retrogradation may be divided into two

281 stages i.e. fast and slow stages.

282 Fig. 3 (b) shows scores plot of PCA based on Raman spectra. All retrogradation

283 starch samples were divided into three categories. The three categories were not

284 completely separated. s. One of categories located at the middle of the scores plot

285 contained retrogradation starch samples stored for 0, 1, 2, and 3d. The retrogradation

286 starch samples stored 4 and 5 days belonged to the second category and the other

287 retrogradation starch samples (stored 10, 15 and 20 day) constituted the third

288 category. In the first category, the retrogradation starch stored for 0, 1and 3 d were

289 separated well from the each other except of 2 d overlapping with 1d. According to

290 the results by enzymatic method the RD of them were increased rapidly. The structure

291 or component of retrogradation starch was very fast at the first three days. For the

292 retrogradation starch samples stored for 4 and 5 days, the RD of them is increased

293 more slowly than the retrogradation starch sample stored 0, 1, 2, and 3 d. The change

294 of retrogradation starch was slow. The RD of retrogradation starch stored for 10, 15

295 and 20 days showed subtle difference by enzymatic method indicating that starch

296 changed very slowly. Structure and component of retrogradation starch were

297 beginning to stabilize. The aggregation of starch samples maybe led by their similar

298 component and structure. The starch retrogradation may be divided into three stage,

299 i.e. fast, slow and stable stage. The stage retrogradation starch categories could be

300 discriminated by PCA. Whereas, the specific RD in starch sample was not

16

301   determined. Therefore, the RD in starch would be determined in following research.
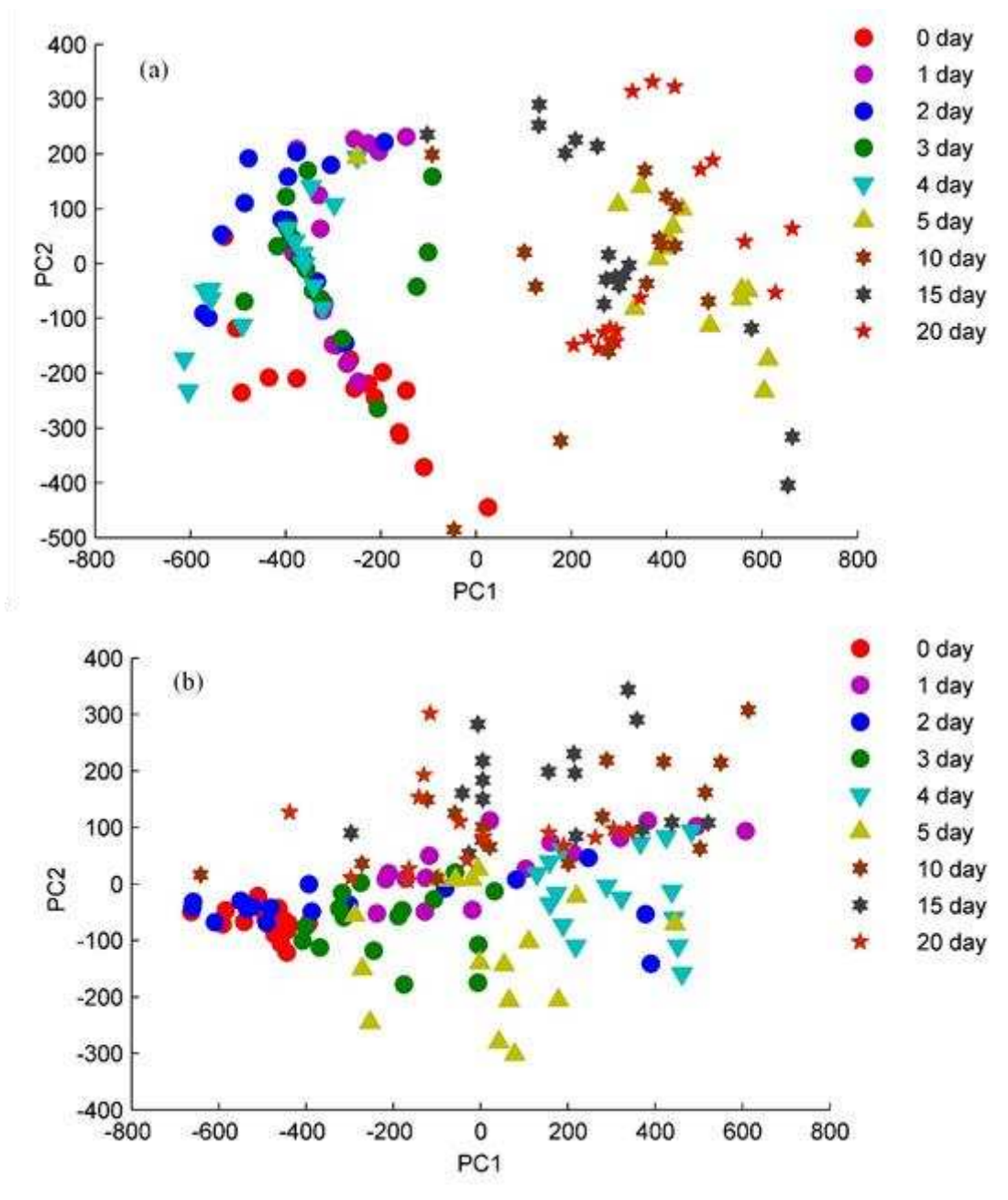
302

303   Fig. 3 score plot of the first principal component (PC1) versus the second principal

304   component (PC2) of different retrogradation starch samples: (a) MIR and (b) Raman

305   **Models for determining RD**

306   **Results of models based on MIR or Raman spectra**

307   PLS, iPLS, siPLS and biPLS algorithm was used in this paper for establishing

17

308 models to determine RD in starch. The results of models based on MIR and Raman

309 spectra were listed in Table 2. From Table 2, good performance was obtained from

310 the PLS models based on MIR or Raman spectra. The prediction values of RD were

311 between 10%~100%. The lowest *RMSECV* value (8.4) was achieved by biPLS

312 model based on Raman spectra. The corresponding correlation coefficient (R_p) of

313 prediction set was 0.9252 which achieved the best performance. The worst model

314 was iPLS model with highest *RMSECV* of based on the single interval in Raman

315 spectra. The optimal Raman spectral interval is the sixth interval in the spectral range

316 of 407 and 485 cm^{-1} when the whole spectrum split into 40 intervals. The

317 characteristic interval variables were attributed to skeletal mode in starch. The MIR

318 biPLS model based on intervals numbered 2, 40, 28, 34, 17, 33, 37, 35, and 38

319 achieved the best performance in all models of MIR. The selected intervals are

320 located in the spectral ranges of 734-817, 3917-4000, 2911-2994, 3413-3497, 1989-

321 2072, 3330-3413, 3665-3749, 3497-3581, 3749-3832 cm^{-1} (Fig. 4 (a)). Fig. 4 (b)

322 shows a correlation between RD measured by reference analysis and RD predicted

323 by MIR biPLS in prediction set. For models of Raman, biPLS models also showed

324 the best performance. The selected Raman intervals were numbered 1 2 5 6 9 10 15

325 33 37 38, corresponding to the wavenumbers in the range of 100-254, 410-564, 718-

326 872, 1181-1258, 2570-2647, 2878-3033 cm^{-1} shown in Fig.5 (a). Fig. 5 (b) shows a

327 correlation between RD measured by reference analysis and RD predicted by Raman

328 biPLS in prediction set.

329   Comparing the models based on MIR and Raman spectra, models based on

330   Raman spectra were better than models based on MIR spectra except iPLS model.

331   IPLS algorithm caused a decline of the model performance when applied to Raman

332   spectra in comparison with full spectrum PLS model. The superiority of Raman

333   spectroscopy may be attributed to specificity and sensitivity (Yuan et al. 2017). The

334   two methods do not offer the identical information about the molecular vibrations and

335   structure. MIR spectroscopy probe the molecular vibrations when the electrical dipole

336   moment changes, while Raman spectroscopy detect molecular vibrations according to

337   the changes of electrical polarizability (Thygesen et al. 2003). The difference between

338   them indicates that molecules tend to be more sensitive to Raman spectroscopy than

339   to MIR spectroscopy. For instance, the C-C or C=C bond is more sensitive to Raman

340   spectroscopy than to MIR spectroscopy. According to the characteristic vibrational

341   bands for MIR and Raman found in food system, the skeletal mode of starch lead to

342   specific vibrations in the Raman spectral regions located at 900-800 and 500-400 cm^{-1}

343   (Thygesen et al. 2003). MIR is strongly dependent on proper sample preparation and

344   moisture content can seriously affect MIR spectra. Conversely, Raman is highly

345   sensitive and do not require special sample treatment.
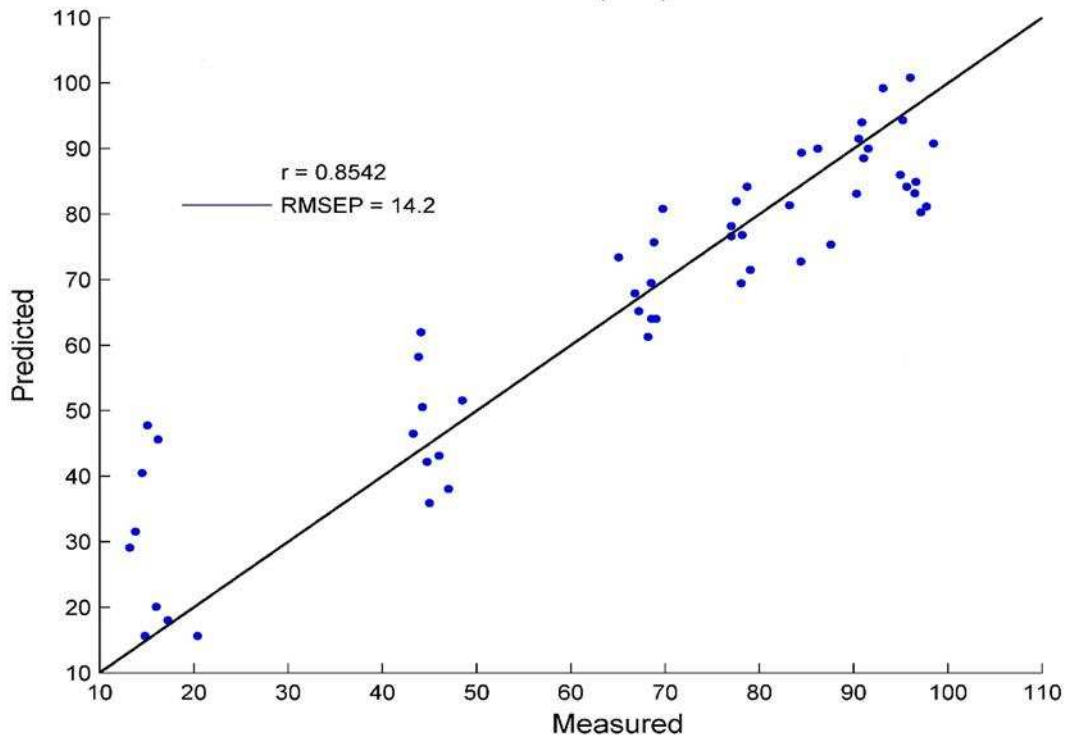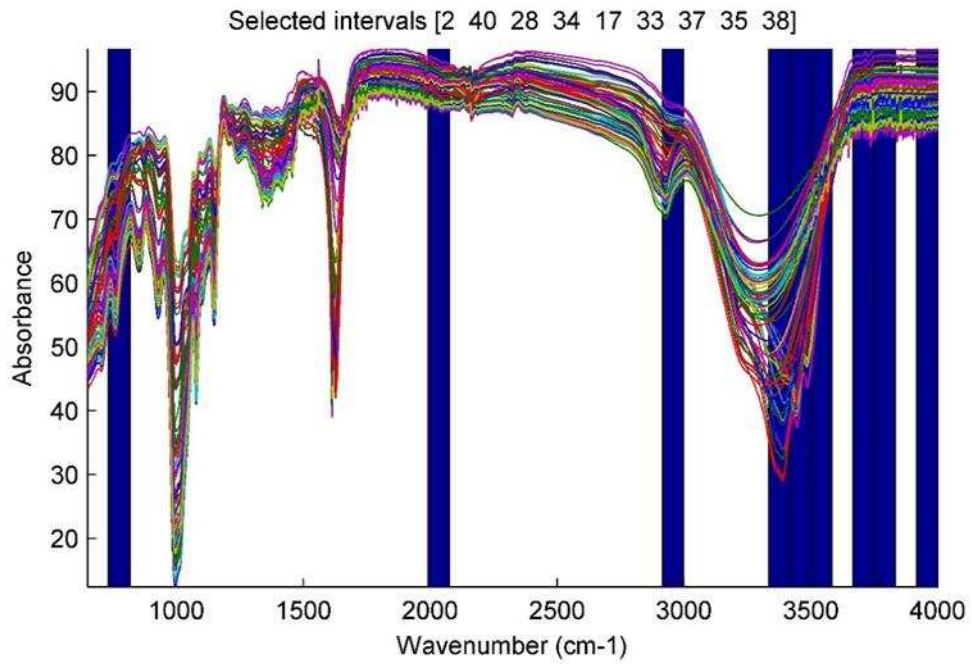
346

347   Fig. 4 (a): the efficient intervals of MIR variables selected by biPLS for predicting RD

348   and (b): reference measured values versus MIR predictive values of RD predicted by

349   biPLS in prediction set
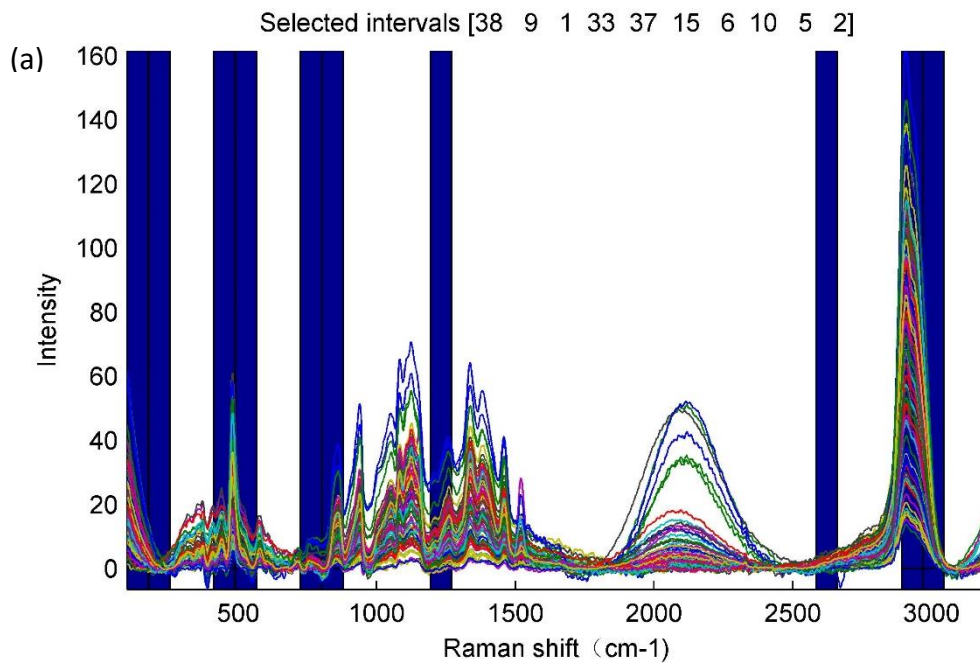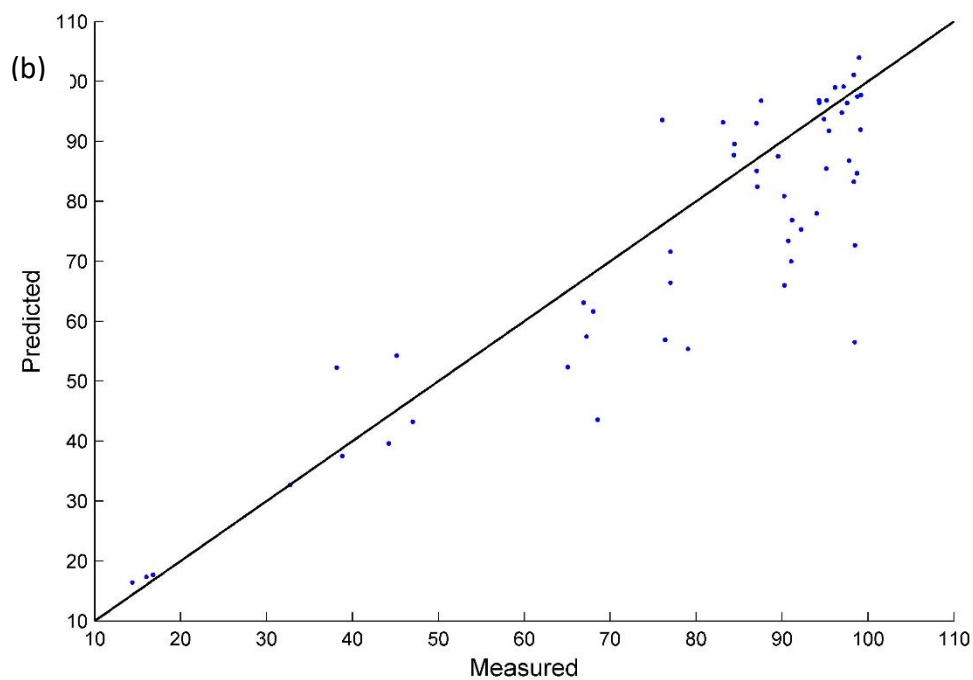
Fig. 5 (a): the efficient intervals of Raman variables selected by biPLS for predicting RD and (b): reference measured values versus Raman predictive values of RD predicted by biPLS in prediction set.

Results of models based on fusion data

The validity of data fusion method has been demonstrated in the literature. Even

though the performance of models based on MIR or Raman spectra is satisfied, the

models based on information extracted from MIR and Raman spectra were still

359   established for verifying that Raman with aid of MIR would be better than Raman

360   spectroscopy.

361   As listed in Table 2, the prediction performance of PLS model based on low-

362   level data is not improved in comparison with that of models based on MIR or

363   Raman. Our findings are in agreement with results obtained by other researchers

364   (Nunes et al. 2016). This might be due to that the fusion data from MIR and Raman

365   spectra contained too much redundant information which significantly result in

366   decline of PLS model performance.

367   To overcome too much redundant information, characteristic intervals of MIR

368   and Raman which selected by biPLS in section 3.4.1 were merged as medium-level

369   fusion data. The process of medium-level data fusion was shown in Fig. 6. As a result,

370   PLS model based on characteristic intervals of MIR and Raman (medium-level fusion

371   data) achieved a better performance with the highest R_p of 0.9658 than PLS model

372   based on full raw variables (low-level fusion data). Low-level fusion is simple, just

373   uses merge raw spectra. But high data volume may contain a large number of noise or

374   irrelevant information. The performance of predictive models would be influenced by

375   the negative information. Some limitation of low-level fusion can be partially

376   overcome by medium-level fusion. Characteristic intervals can decrease the data

377   volume and eliminate noise or irrelevant information.

378   Retrogradation degree are determined only by Raman spectroscopy, and satisfied

379   results are obtained. (Table 2). But by combining MIR and Raman spectroscopy, more

22

380   accurate and reliable models were obtained. The combination of MIR and Raman

381   spectroscopy proved better in determination of retrogradation degree compared to

382   single Raman spectroscopy. Though Raman spectroscopy and chemometric tools have

383   been successfully used for exploratory analysis of pure corn, cassava starch samples

384   and mixtures of both starches, as well as for the quantification of amylose content in

385   corn and cassava starch samples (Almeida et al. 2010). Both MIR and Raman can

386   generate bands linked to fundamental vibration and supply fingerprints of components

387   that can be used for quantitative and qualitative characterization. Even though both

388   methods probe molecular vibrations and structure, they do not provide exactly the

389   same information (Thygesen et al. 2003). Raman spectroscopy detect molecular

390   vibrations according to the changes of electrical polarizability. While MIR

391   spectroscopy probe the molecular vibrations when the electrical dipole moment

392   changes. They are complementary techniques for the study of molecular vibrations

393   and structure. For example, the C-C group has a strong Raman scattering band in

394   Raman spectra but weak absorption bands in the mid-infrared. O–H vibration is very

395   strong in MIR, but very weak in Raman(Yang and Irudayaraj 2002). The intensities of

396   characteristic bands in Raman and MIR spectra collected from same food are different

397   and the information they contain are not identical (Flores-Morales et al. 2012). Due to

398   their distinct advantages, data fusion, as an emerging technology, is an efficient way

399   for the optimum utilization of data from different sources, and has been successfully

400   used to the rapid measurement of retrogradation starch in this paper. Therefore, a

401   useful methods based on MIR and Raman spectroscopy were developed for

402   determining retrogradation starch.
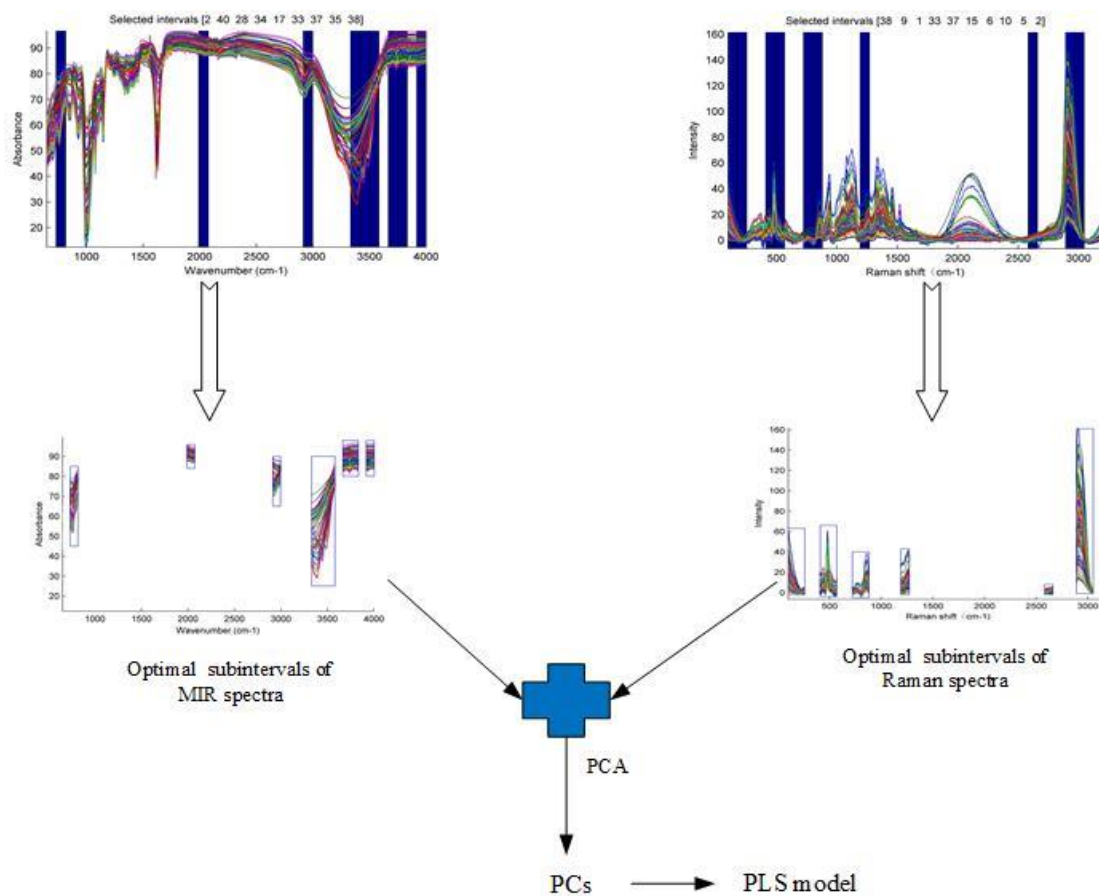
403

404   Fig. 6 PLS model based on medium fusion data extracted from the MIR and Raman

405   spectra.

406   Table 2 the results of different predictive models

Spectra	Models	LV	Calibration set		Prediction set	
			RMSECV	Rc	RMSEP	Rp
MIR spectra	WS-PLS	10	12.8	0.8956	16.2	0.8162
	iPLS	7	14.3	0.8538	16.5	0.8101
	siPLS	8	11.5	0.9016	15.1	0.8401
	biPLS	8	10.0	0.9258	14.2	0.8542
Raman spectra	WS-PLS	10	12.9	0.8924	15.9	0.8204
	iPLS	5	14.9	0.8433	17.1	0.808
	siPLS	7	10.0	0.9275	13.5	0.8806
	biPLS	8	8.4	0.9587	10.1	0.9252
Fusion spectra	low-PLS	12	7.2	0.9873	8.7	0.9573
	medium-PLS	7	7.0	0.9887	7.7	0.9658

Conclusion

The RD in starch stored for different storage time have been predicated by MIR and Raman spectroscopy combined with chemometrics. The PLS model based on medium-level fusion data of MIR and Raman spectra had the best prediction performance with correlation coefficient (R) of 0.9658. Retrogradation starch was obtained by chilling gelatinized corn starch for different time (0, 1, 2, 3, 4, 5, 10, 15, 20 days). The low-level and medium-level fusion data extracted from MIR and Raman were also analyzed by PLS. In addition, The MIR and Raman spectra of retrogradation starch were analyzed by SG, PCA, PLS, iPLS, siPLS and biPLS for determination of RD in starch. The results demonstrated that the prediction performance of models for Raman are better than those based on the MIR except iPLS model. Variables selection improved the performance of PLS models. PLS model based on medium-level fusion data achieved the best performance in comparison with the models. Prediction of the RD in starch based on combination of MIR and Raman

422 spectroscopy are more accurately than that based on single technique. This indicates

423 that the developed methodology may be able to forecast the quality, acceptability and

424 shelf-life of starch products or starch-containing products easily damaged by starch

425 retrogradation.

426 **Acknowledgement**

439 **Compliance with Ethical Standards**

440 **Conflict of Interest** The authors declare that they have no conflict of interest.

441 **Ethical Approval** This article does not contain any studies with human participants or

442 animals performed by any of the authors.

443   **Informed Consent** Informed consent is not applicable for the nature of this study.

444   **Reference**

445   Almeida MR, Alves RS, Nascimbem LBLR, Stephani R, Poppi RJ, de Oliveira LFC (2010) Determination of
446   amylose content in starch using Raman spectroscopy and multivariate calibration analysis
447   Analytical and Bioanalytical Chemistry 397:2693-2701 doi:10.1007/s00216-010-3566-2

448   Baranska M, Schulz H, Baranski R, Nothnagel T, Christensen LP (2005) In Situ Simultaneous Analysis of
449   Polyacetylenes, Carotenoids and Polysaccharides in Carrot Roots Journal of Agricultural and
450   Food Chemistry 53:6565-6571 doi:10.1021/jf0510440

451   Borràs E, Ferré J, Boqué R, Mestres M, Aceña L, Bust o O (2015) Data fusion methodologies for food
452   and beverage authentication and quality assessment – A review Analytica Chimica Acta
453   891:1-14 doi:http://dx.doi.org/10.1016/j.aca.2015.04.042

454   Chang S-M, Liu L-C (1991) Retrogradation of Rice Starches Studied by Differential Scanning Calorimetry
455   and Influence of Sugars, NaCl and Lipids Journal of Food Science 56:564-566
456   doi:10.1111/j.1365-2621.1991.tb05325.x

457   Chen H, Pan T, Chen J, Lu Q (2011) Waveband selection for NIR spectroscopy analysis of soil organic
458   matter based on SG smoothing and MWPLS methods Chemometrics and Intelligent
459   Laboratory Systems 107:139-146 doi:http://dx.doi.org/10.1016/j.chemolab.2011.02.008

460   Chen Q, Zhao J, Liu M, Cai J, Liu J (2008) Determination of total polyphenols content in green tea using
461   FT-NIR spectroscopy and different PLS algorithms Journal of Pharmaceutical and Biomedical
462   Analysis 46:568-573 doi:http://dx.doi.org/10.1016/j.jpba.2007.10.031

463   de Peinder P, Vredenbregt MJ, Visser T, de Kaste D (2008) Detection of Lipitor® counterfeits: A
464   comparison of NIR and Raman spectroscopy in combination with chemometrics Journal of
465   Pharmaceutical and Biomedical Analysis 47:688-694
466   doi:http://dx.doi.org/10.1016/j.jpba.2008.02.016

467   Di Paola RD, Asis R, Aldao MAJ (2003) Evaluation of the Degree of Starch Gelatinization by a New
468   Enzymatic Method Starch - Stärke 55:403-409 doi:10.1002/star.200300167

469   Eliasson AC (2010) Gelatinization and retrogradation of starch in foods and its implications for food
470   quality. In: Skibsted LH, Risbo J, Andersen ML (eds) Chemical deterioration and physical
471   instability of food and beverages. Woodhead Publishing Limited, Oxford, U.K., pp 296-323

472   Ferrero C, Martino MN, Zaritzky NE (1994) Corn Starch-Xanthan Gum Interaction and Its Effect on the
473   Stability During Storage of Frozen Gelatinized Suspension Starch - Stärke 46:300-308
474   doi:10.1002/star.19940460805

475   Flores-Morales A, Jiménez-Estrada M, Mora-Escobedo R (2012) Determination of the structural
476   changes by FT-IR, Raman, and CP/MAS 13C NMR spectroscopy on retrograded starch of maize
477   tortillas Carbohydrate Polymers 87:61-68
478   doi:http://dx.doi.org/10.1016/j.carbpol.2011.07.011

479   Haiyan Y, Xiaoying N, Yibin Y, Xingxiang P (2008) Non-invasive determination of enological parameters
480   of rice wine by Vis-NIR spectroscopy and least-squares support vector machines. Paper
481   presented at the 2008 Providence, Rhode Island, June 29 – July 2, 2008, St. Joseph, Mich.,

482   Hayakawa K, Tanaka K, Nakamura T, Endo S, Hoshino T (1997) Quality Characteristics of Waxy

Hexaploid Wheat (Triticum aestivum L.): Properties of Starch Gelatinization and Retrogradation Cereal Chemistry Journal 74:576-580 doi:10.1094/CCHEM.1997.74.5.576

Karim AA, Norziah MH, Seow CC (2000) Methods for the study of starch retrogradation Food Chem 71:9-36 doi:http://dx.doi.org/10.1016/S0308-8146(00)00130-8

Kim J-O, Kim W-S, Shin M-S (1997) A Comparative Study on Retrogradation of Rice Starch Gels by DSC, X-Ray and α-Amylase Methods Starch - Stärke 49:71-75 doi:10.1002/star.19970490207

Kizil R, Irudayaraj J, Seetharaman K (2002) Characterization of Irradiated Starches by Using FT-Raman and FTIR Spectroscopy Journal of Agricultural and Food Chemistry 50:3912-3918 doi:10.1021/jf011652p

Lin Y-W, Deng B-C, Wang L-L, Xu Q-S, Liu L, Liang Y-Z (2016) Fisher optimal subspace shrinkage for block variable selection with applications to NIR spectroscopic analysis Chemometrics and Intelligent Laboratory Systems 159:196-204 doi:http://dx.doi.org/10.1016/j.chemolab.2016.11.002

Liu H, Yu L, Chen L, Li L (2007) Retrogradation of corn starch after thermal treatment at different temperatures Carbohydrate Polymers 69:756-762 doi:http://dx.doi.org/10.1016/j.carbpol.2007.02.011

Ma H-l, Wang J-w, Chen Y-j, Cheng J-l, Lai Z-t (2017) Rapid authentication of starch adulterations in ultrafine granular powder of Shanyao by near-infrared spectroscopy coupled with chemometric methods Food Chem 215:108-115 doi:http://dx.doi.org/10.1016/j.foodchem.2016.07.156

Mahdad-Benzerdjeb A, Taleb-Mokhtari IN, Sekkal-Rahal M (2007) Normal coordinates analyses of disaccharides constituted by d-glucose, d-galactose and d-fructose units Spectrochimica Acta Part A: Molecular and Biomolecular Spectroscopy 68:284-299 doi:http://dx.doi.org/10.1016/j.saa.2006.11.032

Mariotti M, Sinelli N, Catenacci F, Pagani MA, Lucisano M (2009) Retrogradation behaviour of milled and brown rice pastes during ageing Journal of Cereal Science 49:171-177 doi:http://dx.doi.org/10.1016/j.jcs.2008.09.005

Monakhova YB, Diehl BWK (2016) Authentication of the origin of sucrose-based sugar products using quantitative natural abundance 13C NMR Journal of the Science of Food and Agriculture 96:2861-2866 doi:10.1002/jsfa.7456

Nørgaard L, Saudland A, Wagner J, Nielsen JP, Munck L, Engelsen SB (2000) Interval Partial Least-Squares Regression (iPLS): A Comparative Chemometric Study with an Example from Near-Infrared Spectroscopy Applied Spectroscopy 54:413-419

Nikonenko NA, Buslov DK, Sushko NI, Zhbankov RG (2005) Spectroscopic manifestation of stretching vibrations of glycosidic linkage in polysaccharides Journal of Molecular Structure 752:20-24 doi:http://dx.doi.org/10.1016/j.molstruc.2005.05.015

Nunes KM, Andrade MVO, Santos Filho AMP, Lasmar MC, Sena MM (2016) Detection and characterisation of frauds in bovine meat in natura by non-meat ingredient additions using data fusion of chemical parameters and ATR-FTIR spectroscopy Food Chem 205:14-22 doi:http://dx.doi.org/10.1016/j.foodchem.2016.02.158

Olayinka OO, Olu-Owolabi BI, Adebowale KO (2011) Effect of succinylation on the physicochemical, rheological, thermal and retrogradation properties of red and white sorghum starches Food

525   Hydrocolloids 25:515-520 doi:http://dx.doi.org/10.1016/j.foodhyd.2010.08.002

526 Paker I, Matak KE (2016) Influence of pre-cooking protein paste gelation conditions and post-cooking

527   gel storage conditions on gel texture Journal of the Science of Food and Agriculture 96:280-

528   286 doi:10.1002/jsfa.7091

529 Rocha JTC et al. (2016) Sulfur Determination in Brazilian Petroleum Fractions by Mid-infrared and

530   Near-infrared Spectroscopy and Partial Least Squares Associated with Variable Selection

531   Methods Energy & Fuels 30:698-705 doi:10.1021/acs.energyfuels.5b02463

532 Romano G, Nagle M, Müller J (2016) Two-parameter Lorentzian distribution for monitoring physical

533   parameters of golden colored fruits during drying by application of laser light in the Vis/NIR

534   spectrum Innovative Food Science & Emerging Technologies 33:498-505

535   doi:http://dx.doi.org/10.1016/j.ifset.2015.11.007

536 Sajilata MG, Singhal RS, Kulkarni PR (2006) Resistant Starch–A Review Comprehensive Reviews in Food

537   Science and Food Safety 5:1-17 doi:10.1111/j.1541-4337.2006.tb00076.x

538 Smits ALM, Ruhnau FC, Vliegenthart JFG, van Soest JJG (1998) Ageing of Starch Based Systems as

539   Observed with FT-IR and Solid State NMR Spectroscopy Starch - Stärke 50:478-483

540   doi:10.1002/(SICI)1521-379X(199812)50:11/12<478::AID-STAR478>3.0.CO;2-P

541 Synytsya A, ČopíKová J, Matějka P, Machovič V (2003) Fourier transform Raman and infrared

542   spectroscopy of pectins Carbohydrate Polymers 54:97-106

543 Thygesen LG, Løkke MM, Micklander E, Engelsen SB (2003) Vibrational microspectroscopy of food.

544   Raman vs. FT-IR Trends in Food Science & Technology 14:50-57

545   doi:http://dx.doi.org/10.1016/S0924-2244(02)00243-1

546 Vankeirsbilck T, Vercauteren A, Baeyens W, Van der Weken G, Verpoort F, Vergote G, Remon JP (2002)

547   Applications of Raman spectroscopy in pharmaceutical analysis TrAC Trends in Analytical

548   Chemistry 21:869-877 doi:http://dx.doi.org/10.1016/S0165-9936(02)01208-6

549 Varliklioz Er S, Eksi-Kocak H, Yetim H, Boyaci IH (2016) Novel Spectroscopic Method for Determination

550   and Quantification of Saffron Adulteration Food Analytical Methods:1-9 doi:10.1007/s12161-

551   016-0710-4

552 Winter WT, Kwak YT (1987) Rapid-scanning Raman spectroscopy: a novel approach to starch

553   retrogradation Food Hydrocolloids 1:461-463 doi:http://dx.doi.org/10.1016/S0268-

554   005X(87)80041-3

555 Wu Z, Xu E, Long J, Pan X, Xu X, Jin Z, Jiao A (2016) Comparison between ATR-IR, Raman, concatenated

556   ATR-IR and Raman spectroscopy for the determination of total antioxidant capacity and total

557   phenolic content of Chinese rice wine Food Chem 194:671-679

558   doi:http://dx.doi.org/10.1016/j.foodchem.2015.08.071

559 Xu W, Liu X, Xie L, Ying Y (2014) Comparison of Fourier Transform Near-Infrared, Visible Near-Infrared,

560   Mid-Infrared, and Raman Spectroscopy as Non-Invasive Tools for Transgenic Rice

561   Discrimination Transactions of the Asabe 57:141-150

562 Yang L, Zhang L-M (2009) Chemical structural and chain conformational characterization of some

563   bioactive polysaccharides isolated from natural sources Carbohydrate Polymers 76:349-361

564   doi:http://dx.doi.org/10.1016/j.carbpol.2008.12.015

565 Yeung KY, Ruzzo WL (2001) Principal component analysis for clustering gene expression data

566   Bioinformatics 17:763-774 doi:10.1093/bioinformatics/17.9.763

567   Yuan J et al. (2017) A rapid Raman detection of deoxynivalenol in agricultural products Food Chem

568   221:797-802 doi:http://dx.doi.org/10.1016/j.foodchem.2016.11.101

569   Zou X, Zhao J, Li Y (2007) Selection of the efficient wavelength regions in FT-NIR spectroscopy for

570   determination of SSC of 'Fuji' apple based on BiPLS and FiPLS models Vibrational

571   Spectroscopy 44:220-227 doi:http://dx.doi.org/10.1016/j.vibspec.2006.11.005

572

573